PCCP

Gas Phase Formation of Cyclopentanaphthalene (Benzindene) Isomers via Reactions of 5- and 6-Indenyl Radicals with Vinylacetylene

Journal:	*Physical Chemistry Chemical Physics*
Manuscript ID	CP-ART-07-2020-003846.R1
Article Type:	Paper
Date Submitted by the Author:	18-Sep-2020

Complete List of Authors:	Zhao, Long; University of Hawaii at Manoa, Department of Chemistry Kaiser, Ralf; University of Hawaii, Lu, Wenchao; b. Chemical Sciences Division, Lawrence Berkeley National Laboratory, Kostko, Oleg; Lawrence Berkeley National Laboratory, Chemical Sciences Division Ahmed, Musahid; Lawrence Berkeley National Laboratory, Chemical Sciences Division Evseev, Mikhail; Samara National Research University Bashkirov, Eugene; Samara National Research University, General and Theoretical Physics Oleinikov, Artem; Samara National Research University Azyazov, Valeriy; Samara National Research University; Lebedev Physical Institute of RAS, Department of Chemical & Electric Discharge Lasers Mebel, Alexander; Florida International University, Chemistry and Biochemistry Howlader, A. Hasan; Florida International University, Department of Chemistry and Biochemistry Wnuk, Stanislaw; Florida International University, Chemistry and Biochemistry

SCHOLARONE™
Manuscripts

Gas Phase Formation of Cyclopentanaphthalene (Benzindene) Isomers via Reactions of 5- and 6-Indenyl Radicals with Vinylacetylene

Long Zhao[1], Ralf I. Kaiser[1*]
[1] Department of Chemistry, University of Hawaii at Manoa, Honolulu, Hawaii, 96822 (USA)

Wenchao Lu[2], Oleg Kostko[2], Musahid Ahmed[2*]
[2] Chemical Sciences Division, Lawrence Berkeley National Laboratory, Berkeley, CA 94720 (USA)

Mikhail M. Evseev,[3] Eugene K. Bashkirov[3]
[3]Samara National Research University, Samara 443086, Russian Federation

Artem D. Oleinikov[3,4], Valeriy N. Azyazov[3,4]
[3]Samara National Research University, Samara 443086, Russian Federation
[4]Lebedev Physical Institute, Samara 443011

Alexander M. Mebel[3,5]* A. Hasan Howlader,[5] Stanislaw F. Wnuk[5]
[3]Samara National Research University, Samara 443086 (Russian Federation)
[5]Department of Chemistry and Biochemistry, Florida International University, Miami, FL 33199 (USA)

[*] Corresponding author:
Ralf I. Kaiser <ralfk@hawaii.edu>
Musahid Ahmed <mahmed@lbl.gov>
Alexander M. Mebel <mebela@fiu.edu>

Abstract:

The tricyclic polycyclic aromatic hydrocarbons (PAHs) 3*H*-cyclopenta[*a*]naphthalene ($C_{13}H_{10}$), 1*H*-cyclopenta[*b*]naphthalene ($C_{13}H_{10}$) and 1*H*-cyclopenta[*a*]naphthalene ($C_{13}H_{10}$) along with their indene-based bicyclic isomers (*E*)-5-(but-1-en-3-yn-1-yl)-1*H*-indene, (*E*)-6-(but-1-en-3-yn-1-yl)-1*H*-indene, 5-(but-3-ene-1-yn-1-yl)-1*H*-in-dene, and 6-(but-3-ene-1-yn-1-yl)-1*H*-indene were formed via a "directed synthesis" in a high-temperature chemical micro reactor at the temperature of 1300 ± 10 K through the reactions of the 5- and 6-indenyl radicals ($C_9H_7^{\bullet}$) with vinylacetylene (C_4H_4). The isomer distributions were probed utilizing tunable vacuum ultraviolet light by recording the photoionization efficiency curves at mass-to-charge of *m/z* = 166 ($C_{13}H_{10}$) and 167 ($^{13}CC_{12}H_{10}$) of the products in a supersonic molecular beam. The underlying reaction mechanisms involve the initial formation of van-der-Waals complexes followed by addition of the 5- and 6-indenyl radicals to vinylacetylene via submerged barriers, followed by isomerization (hydrogen shifts, ring closures), and termination via atomic hydrogen elimination accompanied by aromatization. All the barriers involved in the formation of 3*H*-cyclopenta[*a*]naphthalene, 1*H*-cyclopenta[*b*]naphthalene and 1*H*-cyclopenta[*a*]naphthalene are submerged with respect to the reactants indicating that the mechanisms are in fact barrierless, potentially forming PAHs via the hydrogen abstraction – vinylacetylene addition (HAVA) pathway in the cold molecular clouds such as Taurus Molecular Cloud-1 (TMC-1) at temperatures as low as 10 K.

1. INTRODUCTION

Polycyclic aromatic hydrocarbons (PAHs) carrying five membered rings such as fluorene ($C_{13}H_{10}$) and cyclopentanaphthalenes ($C_{13}H_{10}$) represent fundamental molecular building blocks of non-planar PAHs like corannulene ($C_{20}H_{10}$) along with fullerenes (C_{60}, C_{70}) (Scheme 1).[1-5] These species necessitate five-membered rings in the carbon backbone of the PAH to 'curve' planar PAHs out of the plane. An intimate knowledge of the elementary mechanisms forming PAHs carrying five-membered ring(s) is therefore critical in aiding our understanding of the early stage chemistry in combustion systems as to how precursor PAHs lead to three dimensional (bowl-shaped) carbonaceous structures and ultimately soot particles. However, the elementary steps, chemical dynamics, and reaction mechanisms to form PAHs carrying five-membered ring(s) on the molecular level are largely elusive as detailed synthetic routes have not been investigated comprehensively to date. The presence of five-membered rings in PAHs is also important from the viewpoint of molecular mass growth processes and ring expansion pathways.[6] In combustion flames, ubiquitous open shell reactants such as atomic hydrogen can easily abstract a hydrogen atom from the CH_2 moiety of, e.g. the five-membered ring of indene resulting in the 1-indenyl radical. The radical-radical reaction with a methyl radical has been revealed to lead via ring expansion from a five- to a six-membered ring thus effectively converting molecular building blocks relevant to the formation of three-dimensional carbonaceous nanostructures to those of critical importance to graphene-type two-dimensional nano-sheets at elevated temperatures.[6]

Previously, the simplest prototype of a PAH carrying a single six and five membered ring – indene (C_9H_8) (Scheme 1) has been synthesized under single collision conditions exploiting a crossed molecular beams machine via the reactions of phenyl radicals ($C_6H_5^{\bullet}$) with allene (H_2CCCH_2) and methylacetylene (CH_3CCH) along with their (partially) deuterated counterparts (Scheme 2).[7-11] After overcoming barriers to addition of the phenyl radical to the π-electron density of methylacetylene or allene of 1 to 26 kJ mol^{-1}, the initial collision complexes isomerize predominantly via hydrogen shifts and ring closures followed ultimately by atomic hydrogen loss accompanied by aromatization and indene formation (Scheme 2).[12] These findings were confirmed in recent studies exploiting a micro reactor coupled with vacuum ultraviolet (VUV) photoionization of the neutral reaction products leading to the isomer-selective identification of indene along with its phenylallene, 1-phenyl-1-propyne, and 3-phenyl-1-propyne isomers.[10]

Alternatively, chemical micro reactor studies revealed that indene can also be synthesized at elevated temperatures of 600 ± 100 K exclusively through the reaction of the resonantly stabilized, aromatic benzyl radical ($C_7H_7^{\bullet}$) with acetylene (C_2H_2) after overcoming a significant barrier to addition of 51 kJ mol^{-1} followed by ring closure and hydrogen atom elimination, [13] i.e. a derivative of the Hydrogen-Abstraction-aCetylene-Addition (HACA) mechanism. These C6-C3 and C7-C2 pathways effectively lead to ring annulation to an existing C6-benzene-type ring.[12]

HACA is also implicated in the reaction of the 2-naphthyl radical ($C_{10}H_7^{\bullet}$) with allene (H_2CCCH_2) and methylacetylene (CH_3CCH) leading to 3*H*-cyclopenta[*a*]naphthalene ($C_{13}H_{10}$) and 1*H*-cyclopenta[*b*]naphthalene ($C_{13}H_{10}$) (Scheme 2).[14] However, 1*H*-cyclopenta [*a*]naphthalene was not reported in the study due to low yields. Previous experimental and theoretical investigations also suggested that 3*H*-cyclopenta[*a*]naphthalene can be synthesized from 1-methylnaphthalene ($C_{11}H_{10}$) via hydrogen abstraction from the methyl group followed by acetylene addition reaction, isomerization, and hydrogen elimination (HACA).[2, 15-25] However, these molecular mass growth processes operate only at elevated temperatures as found in combustion systems and in circumstellar envelopes of Asymptotic Giant Branch (AGB) carbon stars close to the photosphere; entrance barriers to addition of 8 to 11 kJ mol^{-1} would effectively block these reactions at low temperatures such as in molecular clouds, e.g., Taurus Molecular Cloud -1 (TMC-1) (10 K), and in hydrocarbon rich atmospheres of planets and their moons like Saturn's satellite Titan (70 – 200 K).[26] Therefore, as of now, ring annulation sequences resulting in an efficient addition of a five-membered ring to an existing benzene moiety have only been exposed to operate at high temperatures; pathways leading to molecular mass growth processes involving five-membered rings at ultralow temperatures are still elusive.

The elucidation of the hydrogen abstraction – vinylacetylene addition (HAVA) reaction mechanisms has opened up barrier-less low temperature pathways to form PAHs even at temperatures as low at 10 K.[27] In the prototype phenyl ($C_6H_5^{\bullet}$) – vinylacetylene (C_4H_4) system, Parker et al. and Zhao et al. provided compelling evidence via crossed molecular beams and chemical micro reactor studies coupled with electronic structure calculations on the formation of naphthalene ($C_{10}H_8$) plus atomic hydrogen.[28, 29] The reaction is initiated by the formation of a van-der-Waals complex followed by addition of the phenyl radical to the CH_2 moiety of the

vinylacetylene reactant leading to a resonantly stabilized radical intermediate ($C_{14}H_{11}$). Although a barrier to addition of 9 kJ mol^{-1} does exist, the transition state is located below the energy of the separated reactants, and hence the barrier to addition is 'submerged'. The existence of submerged barriers is also important in the formation of methyl-substituted naphthalenes such as 1-methylnaphthalene ($C_{11}H_{10}$) and 2-methylnaphthalene ($C_{11}H_{10}$) as demonstrated through the reactions of *m*- and *p*-tolyl radicals ($C_7H_7^{\bullet}$) with vinylacetylene.[30]

Considering that the HAVA mechanism operates at ultralow temperatures and the fact that substituted phenyl-type radicals such as tolyl also react with vinylacetylene barrierlessly leading to ring annulation of a benzene ring, we explore to what extent the reactions of the 5- and 6-indenyl radicals ($C_9H_7^{\bullet}$) with vinylacetylene lead to effective (barrierless) ring annulation of a benzene ring ultimately leading to prototype tricyclic polycyclic aromatic hydrocarbons (PAHs) carrying two six membered and one five membered ring ($C_{13}H_{10}$) in the gas phase (Scheme 2). The 5- and 6-indenyl radicals ($C_9H_7^{\bullet}$) can be rationalized as 'disubstituted' phenyl radicals, in which the five-membered ring acts as a spectator moiety leading to PAH growth in low temperature environments from aromatic radical reactions with key hydrocarbon molecules (vinylacetylene).[31]

2. EXPERIMENTAL

The experiments were carried out at the Advanced Light Source (ALS), Lawrence Berkeley National Laboratory. A detailed description of the experimental set-up was provided previously.[6, 10, 13, 27, 32-36] Briefly, by studying the reactions of the 5- and 6-indenyl radicals ($C_9H_7^{\bullet}$) with vinylacetylene (C_4H_4; Applied Gas; 5% C_4H_4 seeded in 95 % He) under simulated combustion conditions, we deliver experimental and computational evidence of the molecular growth processes to benzindene ($C_{13}H_{10}$) isomers. In separate experiments, a continuous beam of 5- and 6-indenyl radicals ($C_9H_7^{\bullet}$) was prepared *in situ* through the pyrolysis of the corresponding 5- and 6-iodoindene (C_9H_7I) precursors. The in-house synthesis of both iodoindene precursors is described in the Supplementary Information.[37] In separate experiments, the precursors were seeded in the vinylacetylene/helium carrier gas at an inlet pressure of 300 ± 5 Torr. Control experiments were also performed by just replacing the vinylacetylene/helium gases with pure helium while all the other settings (temperature, pressure) remained identical. The gas mixture was expanded through a 0.1 mm diameter orifice into the high-temperature pyrolytic reactor, i.e.

a resistively heated silicon carbide (SiC) tube with 1.0 mm inner diameter and 20 mm heating length. The SiC tube was held at 1300 ± 10 K as monitored by a Type-C thermocouple attached to the center of the heating area. The residence time in the reactor tube under our experimental condition are up to a few tens of μs,[38, 39] with the number of collisions up to a few hundreds.[39] The products formed in the reactor were expanded supersonically, passed through a 2 mm diameter skimmer located 10 mm downstream of the pyrolytic reactor, and entered into the photoionization chamber housing the Wiley–McLaren reflectron time-of-flight mass spectrometer (ReTOF-MS), which was kept at 10^{-6} Torr during the experiment. The quasi-continuous tunable synchrotron VUV light from ALS intersected the neutral molecular beam perpendicularly in the extraction region of the ReTOF-MS. VUV single photon ionization is essentially a fragment-free ionization technique, which would preserve the original information of the target molecules.[40] The ions of the photoionized molecules were accelerated to the field-free TOF region and then collected by a microchannel plate (MCP) detector in the ReTOF mode. The time-dependent ion signal was amplified by a fast preamplifier and convoluted by a multichannel digitizer card.

Photoionization efficiency (PIE) curves, which report the ion count as a function of photon energy with a step interval of 0.05 eV at a well-defined mass-to-charge ratio (*m/z*), were produced by integrating the signal recorded at the specific *m/z* for the species of interest from 7.30 eV to 10.00 eV and normalized by photon fluxes. Experimentally measured PIE curves are usually used for species identification by fitting the calibration PIE curve(s) of the species of interest linearly. To fit the PIE curve and identify the target products lied at *m/z* = 166 ($C_{13}H_{10}$), the calibration curves of the individual isomers were newly obtained at the photoionization energy from 7.3 to 10.0 eV with the 0.05 eV step interval, as presented in the Supporting Information (Figure S1). Among these isomers, 1*H*-cyclopenta[*a*]naphthalene **(P3)** and the branched molecules [(*E*)-5-(but-1-en-3-yn-1-yl)-1*H*-indene **(P4)**, 5-(but-3-ene-1-yn-1-yl)-1*H*-indene **(P5)**, (*E*)-6-(but-1-en-3-yn-1-yl)-1*H*-indene **(P6)** and 6-(but-3-ene-1-yn-1-yl)-1*H*-indene **(P7)**] were synthesized for the current work,[37] while the PIE calibration curves for 3*H*-cyclopenta[*a*]naphthalene **(P1)**, and 1*H*-cyclopenta[*b*]naphthalene **(P2)** were already measured and taken from our previous study.[14]

3. COMPUTATIONAL

The calculations of the energies and molecular parameters of various intermediates and transition states for the reactions of 5- and 6-indenyl with vinylacetylene occurring on the $C_{13}H_{11}$ potential energy surface (PES), as well as of the reactants and possible products were carried out at the G3(MP2,CC)//B3LYP/6-311G(d,p) level of theory. Within this theoretical scheme, geometries were optimized and vibrational frequencies were calculated using the density functional B3LYP method with the 6-311G(d,p) basis set. Then, single-point total energies were improved using a series of coupled clusters CCSD(T) and second-order Møller-Plesset perturbation theory MP2 calculations, and the final energy was computed as

E[G3(MP2,CC)] = E[CCSD(T)/6-311G(d,p)] + E[MP2/G3Large)] – E[MP2/6-311G(d,p)] + ZPE [B3LYP/6-311G(d,p)][41-43]

The G3(MP2,CC) model chemistry approach normally provides chemical accuracy of 0.01–0.02 Å for bond lengths, 1–2º for bond angles, and 3–6 kJ mol^{-1} for relative energies of hydrocarbons, their radicals, reaction energies, and barrier heights in terms of average absolute deviations.[42] The GAUSSIAN 09[44] and MOLPRO 2010[45] program packages were employed for the ab initio calculations.

4. RESULTS & DISCUSSION

Illustrative mass spectra collected at a photoionization energy of 9.50 eV are presented in Figure 1 for the reactions of 5-indenyl and 6-indenyl with vinylacetylene (Figs. 1b and d) to extract the molecular formulae of the reaction products connected to the formation of benzindene isomers. An analysis of these data discloses the formation of $C_{13}H_{10}$ molecules (166 amu) along with their ^{13}C isotopologues at *m/z* = 167 in both systems. Considering the molecular weight of the reactants and the products, the $C_{13}H_{10}$ isomer(s) are products of the reaction of the 5-/6-indenyl radical with vinylacetylene followed by hydrogen atom elimination. The ion counts at mass-to-charge ratios (*m/z*) of 242 ($C_9H_7I^+$), 115 ($C_9H_7^+$), and 116 ($C_8{}^{13}CH_7^+$, $C_9H_8^+$) are detectable in the control experiments as well and hence cannot be linked to the reaction of 5- or 6-indenyl radicals with vinylacetylene. These species are associated with the 5- and 6-iodoindene precursors (242 amu), 5-/6-indenyl radicals (115 amu), and indene (116 amu) with the indene likely formed through recombination of 5- or 6-indenyl with a hydrogen atom in the reactor.

The investigation of the mass spectra delivered convincing evidence on the formation of $C_{13}H_9$ (165 amu) and $C_{13}H_{10}$ (166 amu) isomer(s) along with their ^{13}C substituted species $C_{12}{}^{13}CH_{10}$ (167 amu) via the reaction of 5-/6-indenyl radicals with vinylacetylene. It is our goal not only to identify the molecular formulae of the reaction products, but also to unravel which isomers are contributing to these mass-to-charge ratios. Thus, an in-depth analysis of the underlying PIE curves of the *m/z* ratios of interest (Fig. 2) is necessary to reveal the isomers produced. PIE curves for other *m/z* ratios are provided in the Supporting Information (Figures S2 and S3). Each PIE curve reports the ion counts at a well-defined *m/z* ratio as a function of the photon energy ranging from 7.30 eV to 10.00 eV (Fig. 2). The shapes of the PIE curves of different $C_{13}H_{10}$ isomers are distinct and therefore unique; these calibration curves were recorded in separate experiments reported in previous works and here.[14] A linear combination of these base functions is used to fit the experimental PIE curves shown for *m/z* = 165, 166, and 167 (Fig. 2). Even after scaling, these calibrated PIE curves are not superimposable suggesting that *m/z* = 165 does not represent a photoionization fragment of *m/z* = 166, but rather distinct isomer(s). Due to the lack of reference PIE curves of any $C_{13}H_9$ isomer, it is not feasible to elucidate its structure(s). Considering a 1.1% natural abundance of ^{13}C, 14.3 % of the ion signal of *m/z* = 165 ($C_{13}H_9^+$) could contribute to ion counts of *m/z* = 166 ($C_{12}{}^{13}CH_9^+$) (Fig. 2). Fitting of the PIE curves at *m/z* = 166 ($C_{12}{}^{13}CH_9^+/C_{13}H_{10}^+$) reveals the formation of seven $C_{13}H_{10}$ isomers: 3*H*-cyclopenta[*a*]naphthalene **(P1)**, 1*H*-cyclopenta[*b*]naphthalene **(P2)**, 1*H*-cyclopenta[*a*]naphthalene **(P3)**, (*E*)-5-(but-1-en-3-yn-1-yl)-1*H*-indene **(P4)**, 5-(but-3-ene-1-yn-1-yl)-1*H*-indene **(P5)**, (*E*)-6-(but-1-en-3-yn-1-yl)-1*H*-indene **(P6),** and 6-(but-3-ene-1-yn-1-yl)-1*H*-indene **(P7)**. The corresponding PIE curves of *m/z* = 167 ($C_{12}{}^{13}CH_{10}^+$) match the linear fit of the aforementioned seven PAH isomers and reveal that ion signal at *m/z* = 167 originate from their ^{13}C-isotoplogue PAHs ($C_{13}H_{10}$). It should be noticed that for the PIE calibration experiments of the branched indene isomers **P4, P5, P6,** and **P7**, only calibration mixtures of (*E*)-5-(but-1-en-3-yn-1-yl)-1*H*-indene **(P4)** and (*E*)-6-(but-1-en-3-yn-1-yl)-1*H*-indene **(P6)** (40:60) as well as 5-(but-3-ene-1-yn-1-yl)-1*H*-indene **(P5)** and 6-(but-3-ene-1-yn-1-yl)-1*H*-indene **(P7)** (40:60) has been synthesized and hence exploited for the calibration curve (Supporting Information). Note that actual product branching ratios could not be derived due to unknown photoionization cross sections for any of the $C_{13}H_{10}$ isomers formed and hence only mechanistic information for five membered PAH ring formation is reported here. For the calibration PIE curves of the tricyclic isomers

cyclopentanaphthalenes (Fig. S1a-S1c), their ionization energies (IEs) lie in the range of 7.5-7.6 eV, which match the onsets of the experimental PIE measurement (7.55 ± 0.05 eV, Fig. 2). While for the branched indene isomers (Fig. S1d-S1e), their IEs are around 7.70 eV. As the photoionization thresholds are specific for individual species,[46] the cyclopentanaphthalene isomers are critical for the fit in the lower photon energy range, especially at the onsets of PIE curves. Moreover, the experimental PIE curves cannot be fit without the calibration curves of the branched isomers at photon energies higher than 7.70 eV. With the fit presented in Fig. 2, it is clear that all the isomers are necessary for the overall fit. However, due to the two component cis/trans mixtures of the branched isomers, it might not be concluded that all branched isomers were detected. As a conclusion, it is tentative to claim that all the four branched indene isomers are produced in this work. But for the tricyclic isomers, they are critical to replicate the experimentally determined PIE curve.

To extract the underlying reaction pathways, the experimental data are corroborated with electronic structure calculations (Figs. 3 and 4). Figure 3 reveals the potential energy surface (PES) for the reaction of 5-indenyl with vinylacetylene. The approach of 5-indenyl to the C4 and C1 carbon atoms of vinylacetylene is dictated by an attractive long range potential and leads to the barrierless formation of van der-Waals-complexes **[i0a]** and **[i0b]** located 10 kJ mol^{-1} and 7 kJ mol^{-1} below the energy of the separated reactants. By overcoming a barrier of 6 kJ mol^{-1} to addition, **[i0a]** isomerizes to intermediate **[i1]**; this complex represents the key intermediate leading to the formation of the benzindene molecules. It should be stressed that a barrier to addition does exist, but this barrier lies below the energy of the separated reactants and hence is called 'submerged barrier'. Therefore, the formation of **[i1]** from the reactants represents essentially a barrierless entrance process. With a hydrogen shift from C4 and C6 of the indenyl moiety to the β position of the branched C4 chain, **[i1]** can isomerize to **[i3]** and **[i6]**, respectively, followed by cyclization processes to intermediates **[i4]** and **[i7]**. Further [1,2]-type hydrogen shifts from CH_2 to the bare carbon atom in the newly formed six-membered ring lead to intermediates [**i5**] and [**i8**], which contain the carbon backbones of the benzindene isomers. Distinct hydrogen atom losses accompanied by aromatization forms 3*H*-cyclopenta [*a*]naphthalene **(P1)** (from **[i5]**) and 1*H*-cyclopenta[*b*]naphthalene **(P2)** (from **[i8]**). Besides the reaction sequences leading to **P1** and **P2**, intermediate **[i1]** can also undergo an immediate hydrogen atom loss to produce (*E*)-5-(but-1-en-3-yn-1-yl)-1*H*-indene **(P4)** by overcoming a

barrier of 168 kJ mol^{-1}. All the barriers in the routes initiated by the van der-Waals complex **[i0a]** lie below the separate reactants. On the other hand, **[i0b]** isomerizes to intermediate **[i2]**, followed by hydrogen atom loss yielding 5-(but-3-ene-1-yn-1-yl)-1*H*-indene **(P5)**. The barrier in the process from **[i0b]** to **[i2]** is 3 kJ mol^{-1} above the separated reactants indicating that this is not a barrierless route thus requiring somewhat elevated temperatures to proceed.

Figure 4 exhibits the PES for the 6-indenyl - vinylacetylene system. The reaction mechanisms are similar to those described in the aforementioned system of 5-indenyl reacting with vinylacetylene. First, two van der-Waals complexes **[i'0a]** (-11 kJ mol^{-1}) and **[i'0b]** (-7 kJ mol^{-1}) are produced via the approach of 5-indenyl to the C4 and C1 atoms of vinylacetylene, respectively. **[i'0a]** isomerizes to intermediate **[i'1]** by overcoming a submerged barrier of 7 kJ mol^{-1}. Followed by isomerization (hydrogen shifts, cyclization) and hydrogen atom elimination, 1*H*-cyclo-penta[*a*]naphthalene **(P3)** and 1*H*-cyclopenta[*b*]naphthalene **(P2)** can be produced via the reaction sequences **[i'1]** → **[i'3]** → **[i'4]** → **[i'5]** → **P5** and **[i'1]** → **[i'6]** → **[i'7]** → **[i'8]** → **P2**, respectively. Alternatively, a hydrogen atom elimination leads **[i'1]** to (*E*)-6-(but-1-en-3-yn-1-yl)-1*H*-indene **(P6)**. In addition, the van der-Waals complex **[i'0b]** may isomerize to **[i'2]** through a barrier of 11 kJ mol^{-1}, followed by hydrogen atom loss leading to 6-(but-3-ene-1-yn-1-yl)-1*H*-indene **(P7)**. This pathway does not represent a barrierless entrance process since the barrier from **[i'0b]** to **[i'2]** lies 4 kJ mol^{-1} above the energy of the separated reactants.

As the experiments were conducted under combustion-like condition at 1300 ± 10 K, the barriers of 3 and 4 kJ mol^{-1} can be easily overcome. Thus, even 5-(but-3-ene-1-yn-1-yl)-1*H*-indene **(P5)** and 6-(but-3-ene-1-yn-1-yl)-1*H*-indene **(P7)**, can be produced. Recall that due to the isomer mixture of (*E*)-5-(but-1-en-3-yn-1-yl)-1*H*-indene **(P4)** and (*E*)-6-(but-1-en-3-yn-1-yl)-1*H*-indene **(P6)** as well as 5-(but-3-ene-1-yn-1-yl)-1*H*-indene **(P5)** and 6-(but-3-ene-1-yn-1-yl)-1*H*-indene **(P7)**, four branched indene molecules are involved in the fits of the PIE curves of the $C_{13}H_{10}$ isomers in both systems. However, based on the theoretical calculations, we may conclude that **P4** and **P5** are only accessible in the 5-indenyl – vinylacetylene system, while **P6** and **P7** may only be formed in the reaction of 6-indenyl with vinylacetylene.

5. CONCLUSION

Our combined experimental and computational studies revealed critical mass growth processes from aromatic aryl radicals (5-indenyl and 6-indenyl) leading to distinct tricyclic PAHs carrying two six- and one five-membered rings: 3*H*-cyclopenta[*a*]naphthalene, 1*H*-cyclopenta[*b*] naphthalene, and 1*H*-cyclopenta[*a*]naphthalene. The underlying reaction mechanisms involve the formation of van-der-Waals complexes and the de-facto barrier-less addition of the carbon-centered radicals of the 5- and 6-indenyl species to the π-electron density of vinylacetylene reactant at the terminal carbon atoms. The resonantly stabilized free radical intermediates formed further isomerize through hydrogen shifts and ring closure; these processes are terminated by atomic hydrogen elimination accompanied by aromatization leading to the tricyclic PAHs in an overall exoergic reaction. The reaction mechanisms essentially mirror the formation of the naphthalene molecule ($C_{10}H_8$) in the phenyl-vinylacetylene system[12, 28, 29] and suggest that the five-membered ring in the indenyl radicals acts as a spectator. These overall routes to these PAHs are essentially barrierless since all the transition states involved are located below the energy of the separated reactants. The submerged barriers represent a crucial prerequisite for a bimolecular reaction to proceed at low temperatures, since any transition state located above the energy of the separated reactants cannot be overcome at low temperatures in cold molecular clouds such as TMC-1 at temperatures as low as 10 K. Here, the hydrogen abstraction – vinylacetylene addition (HAVA) pathway signifies a versatile reaction mechanism to generate benzindene molecules through barrierless, stepwise ring expansion via elementary gas-phase reactions of an aryl radical with vinylacetylene. The aryl radical can be formed inside molecular clouds from the corresponding aromatic precursor via photolysis by an internal ultraviolet field. In circumstellar envelopes of carbon stars and even under combustion conditions with temperatures of up to a few 1,000 K, molecular mass growth processes could also be triggered by HAVA as a facile key mechanism propelling molecular mass growth processes of PAHs. This study potentially suggests that the five-member-ring contained PAHs can lead, via a low-temperature propagation mechanism, to more complex 3D-structured PAHs such as corannulene and even fullerenes observed in the galaxy.

Acknowledgments

This work was supported by the US Department of Energy, Basic Energy Sciences DE-FG02-03ER15411 (experimental studies) and DE-FG02-04ER15570 (computational studies; synthesis of the $C_{13}H_{10}$ isomers) to the University of Hawaii (UH) and Florida International University (FIU), respectively. W.L., O.K., and M.A. are supported by the Director, Office of Science, Office of Basic Energy Sciences, of the U.S. Department of Energy under Contract No. DE-AC02-05CH11231, through the Gas Phase Chemical Physics program of the Chemical Sciences Division. The ALS is supported under the same contract. Ab initio calculations at Samara University were supported by the Ministry of Science and Higher Education of the Russian Federation under Grant No. 14.Y26.31.0020.

Author Contributions

R.I.K. designed the experiment; L.Z., W.L. and O.K. carried out the experimental measurements; M.A. supervised the experiment; L.Z. performed the data analysis; M.M.E., E.K.B., A.D.O., V.N.A. and A.M.M. carried out the theoretical analysis; A.H.H. and S.F.W. synthesized the compounds, A.M.M., and M.A. discussed the data; R.I.K., A.M.M. and L.Z. wrote the manuscript.

References

1. D. Josa, L. Azevedo dos Santos, I. Gonzalez-Veloso, J. Rodriguez-Otero, E. M. Cabaleiro-Lago and T. de Castro Ramalho, *RSC Adv.*, 2014, **4**, 29826-29833.
2. H. Richter, W. J. Grieco and J. B. Howard, *Combust. Flame*, 1999, **119**, 1-22.
3. H. Richter, W. J. Grieco and J. B. Howard, *Chem. Phys. Processes Combust.*, 1997, 135-138.
4. L. Becker and T. E. Bunch, *Meteorit. Planet. Sci.*, 1997, **32**, 479-487.
5. G. Devi, M. Buragohain and A. Pathak, *Planet. Space Sci.*, 2020, **183**, 104593.
6. L. Zhao, R. I. Kaiser, W. Lu, B. Xu, M. Ahmed, A. N. Morozov, A. M. Mebel, A. H. Howlader and S. F. Wnuk, *Nat. Commun.*, 2019, **10**, 1-7.
7. T. Yang, D. S. N. Parker, B. B. Dangi, R. I. Kaiser and A. M. Mebel, *Phys. Chem. Chem. Phys.*, 2015, **17**, 10510-10519.
8. L. Vereecken, H. F. Bettinger and J. Peeters, *Phys. Chem. Chem. Phys.*, 2002, **4**, 2019-2027.
9. L. Vereecken, J. Peeters, H. F. Bettinger, R. I. Kaiser, P. v. R. Schleyer and H. F. Schaefer, III, *J. Am. Chem. Soc.*, 2002, **124**, 2781-2789.
10. F. Zhang, R. I. Kaiser, V. V. Kislov, A. M. Mebel, A. Golan and M. Ahmed, *J. Phys. Chem. Lett.*, 2011, **2**, 1731-1735.
11. D. S. N. Parker, F. Zhang, R. I. Kaiser, V. V. Kislov and A. M. Mebel, *Chem. - Asian J.*, 2011, **6**, 3035-3047.
12. A. M. Mebel, A. Landera and R. I. Kaiser, *J. Phys. Chem. A*, 2017, **121**, 901-926.

13. D. S. N. Parker, R. I. Kaiser, O. Kostko and M. Ahmed, *ChemPhysChem*, 2015, **16**, 2091-2093.
14. L. Zhao, M. Prendergast, R. I. Kaiser, B. Xu, U. Ablikim, W. Lu, M. Ahmed, A. D. Oleinikov, V. N. Azyazov, A. H. Howlader, S. F. Wnuk and A. M. Mebel, *Phys. Chem. Chem. Phys.*, 2019, **21**, 16737-16750.
15. A. Kitajima, T. Hatanaka, M. Takeuchi, H. Torikai and T. Miyadera, *Combust. Flame*, 2005, **142**, 72-88.
16. C. S. McEnally and L. D. Pfefferle, *Combust. Flame*, 2007, **148**, 210-222.
17. V. Kislov and A. Mebel, *J. Phys. Chem.*, 2008, **112**, 700-716.
18. L. Vereecken and J. Peeters, *Phys. Chem. Chem. Phys.*, 2003, **5**, 2807-2817.
19. J. Bittner and J. Howard, *Proc. Combust. Inst.*, 1981, **18**, 1105-1116.
20. J. DeCoster, A. Ergut, Y. A. Levendis, H. Richter, J. B. Howard and J. B. Carlson, *Proc. Combust. Inst.*, 2007, **31**, 491-499.
21. F. Zhang, X. Gu and R. I. Kaiser, *J. Chem. Phys.*, 2008, **128**, 084315.
22. R. Sivaramakrishnan, R. S. Tranter and K. Brezinsky, *J. Phys. Chem.*, 2006, **110**, 9400-9404.
23. M. Frenklach, D. W. Clary, W. C. Gardiner Jr and S. E. Stein, *Proc. Combust. Inst.*, 1988, **21**, 1067-1076.
24. M. Frenklach, T. Yuan and M. Ramachandra, *Energy Fuels*, 1988, **2**, 462-480.
25. V. Kislov and A. Mebel, *J. Phys. Chem.*, 2007, **111**, 3922-3931.
26. R. D. Lorenz and J. I. Lunine, *Planet. Space Sci.*, 1997, **45**, 981-992.
27. L. Zhao, R. I. Kaiser, B. Xu, U. Ablikim, M. Ahmed, M. M. Evseev, E. K. Bashkirov, V. N. Azyazov and A. M. Mebel, *Nat. Astron.*, 2018, **2**, 973.
28. D. S. Parker, F. Zhang, Y. S. Kim, R. I. Kaiser, A. Landera, V. V. Kislov, A. M. Mebel and A. Tielens, *Proc. Natl. Acad. Sci. USA*, 2012, **109**, 53-58.
29. L. Zhao, R. I. Kaiser, B. Xu, U. Ablikim, M. Ahmed, M. V. Zagidullin, V. N. Azyazov, A. H. Howlader, S. F. Wnuk and A. M. Mebel, *J. Phys. Chem. Lett.*, 2018, **9**, 2620-2626.
30. T. Yang, L. Muzangwa, R. I. Kaiser, A. Jamal and K. Morokuma, *Phys. Chem. Chem. Phys.*, 2015, **17**, 21564-21575.
31. F. Zhang, Y. S. Kim, R. I. Kaiser, S. P. Krishtal and A. M. Mebel, *J. Phys. Chem.*, 2009, **113**, 11167-11173.
32. F. Zhang, R. I. Kaiser, A. Golan, M. Ahmed and N. Hansen, *J. Phys. Chem. A*, 2012, **116**, 3541-3546.
33. A. Golan, M. Ahmed, A. M. Mebel and R. I. Kaiser, *Phys. Chem. Chem. Phys.*, 2013, **15**, 341-347.
34. T. Yang, T. P. Troy, B. Xu, O. Kostko, M. Ahmed, A. M. Mebel and R. I. Kaiser, *Angew. Chem. Int. Ed.*, 2016, **55**, 14983-14987.
35. L. Zhao, R. I. Kaiser, B. Xu, U. Ablikim, M. Ahmed, D. Joshi, G. Veber, F. R. Fischer and A. M. Mebel, *Nat. Astron.*, 2018, **2**, 413-419.
36. L. Zhao, R. I. Kaiser, B. Xu, U. Ablikim, W. Lu, M. Ahmed, M. M. Evseev, E. K. Bashkirov, V. N. Azyazov, M. V. Zagidullin, A. N. Morozov, A. H. Howlader, S. F. Wnuk, A. M. Mebel, D. Joshi, G. Veber and F. R. Fischer, *Nat. Commun.*, 2019, **10**, 1510.
37. A. Hasan Howlader, K. Diaz, A. M. Mebel, R. I. Kaiser and S. F. Wnuk, *Tetrahedron Letters*, 2020, DOI: https://doi.org/10.1016/j.tetlet.2020.152427, 152427.

38. Q. Guan, K. N. Urness, T. K. Ormond, D. E. David, G. Barney Ellison and J. W. Daily, *Int. Rev. Phys. Chem.*, 2014, **33**, 447-487.
39. M. V. Zagidullin, R. I. Kaiser, D. P. Porfiriev, I. P. Zavershinskiy, M. Ahmed, V. N. Azyazov and A. M. Mebel, *J. Phys. Chem. A*, 2018, **122**, 8819-8827.
40. F. Qi, *Proc. Combust. Inst.*, 2013, **34**, 33-63.
41. L. A. Curtiss, K. Raghavachari, P. C. Redfern, V. Rassolov and J. A. Pople, *J. Chem. Phys.*, 1998, **109**, 7764-7776.
42. L. A. Curtiss, K. Raghavachari, P. C. Redfern, A. G. Baboul and J. A. Pople, *Chem. Phys. Lett.*, 1999, **314**, 101-107.
43. A. G. Baboul, L. A. Curtiss, P. C. Redfern and K. Raghavachari, *J. Chem. Phys.*, 1999, **110**, 7650-7657.
44. M. J. Frisch, G. W. Trucks, H. B. Schlegel, G. E. Scuseria, M. A. Robb, J. R. Cheeseman, G. Scalmani, V. Barone, B. Mennucci, G. A. Petersson, H. Nakatsuji, M. Caricato, X. Li, H. P. Hratchian, A. F. Izmaylov, J. Bloino, G. Zheng, J. L. Sonnenberg, M. Hada, M. Ehara, K. Toyota, R. Fukuda, J. Hasegawa, M. Ishida, T. Nakajima, Y. Honda, O. Kitao, H. Nakai, T. Vreven, J. A. Montgomery, Jr., J. E. Peralta, F. Ogliaro, M. Bearpark, J. J. Heyd, E. Brothers, K. N. Kudin, V. N. Staroverov, T. Keith, R. Kobayashi, J. Normand, K. Raghavachari, A. Rendell, J. C. Burant, S. S. Iyengar, J. Tomasi, M. Cossi, N. Rega, J. M. Millam, M. Klene, J. E. Knox, J. B. Cross, V. Bakken, C. Adamo, J. Jaramillo, R. Gomperts, R. E. Stratmann, O. Yazyev, A. J. Austin, R. Cammi, C. Pomelli, J. W. Ochterski, R. L. Martin, K. Morokuma, V. G. Zakrzewski, G. A. Voth, P. Salvador, J. J. Dannenberg, S. Dapprich, A. D. Daniels, O. Farkas, J. B. Foresman, J. V. Ortiz, J. Cioslowski and D. J. Fox, Gaussian 09, revision A.02, (Gaussian Inc., CT), 2009.
45. H. J. Werner, P. J. Knowles, G. Knizia, F. R. Manby, M. Schütz, P. Celani, W. Györffy, D. Kats, T. Korona, R. Lindh, A. Mitrushenkov, G. Rauhut, K. R. Shamasundar, T. B. Adler, R. D. Amos, A. Bernhardsson, A. Berning, D. L. Cooper, M. J. O. Deegan, A. J. Dobbyn, F. Eckert, E. Goll, C. Hampel, A. Hesselmann, G. Hetzer, T. Hrenar, G. Jansen, C. Köppl, Y. Liu, A. W. Lloyd, R. A. Mata, A. J. May, S. J. McNicholas, W. Meyer, M. E. Mura, A. Nicklaß, D. P. O'Neill, P. Palmieri, D. Peng, K. Pflüger, R. Pitzer, M. Reiher, T. Shiozaki, H. Stoll, A. J. Stone, R. Tarroni, T. Thorsteinsson and M. Wang, MOLPRO, version 2010.1, http://www.molpro.net, (University College Cardiff Consultants Ltd, United Kingdom), 2010.
46. T. A. Cool, J. Wang, K. Nakajima, C. A. Taatjes and A. Mcllroy, *International Journal of Mass Spectrometry*, 2005, **247**, 18-27.

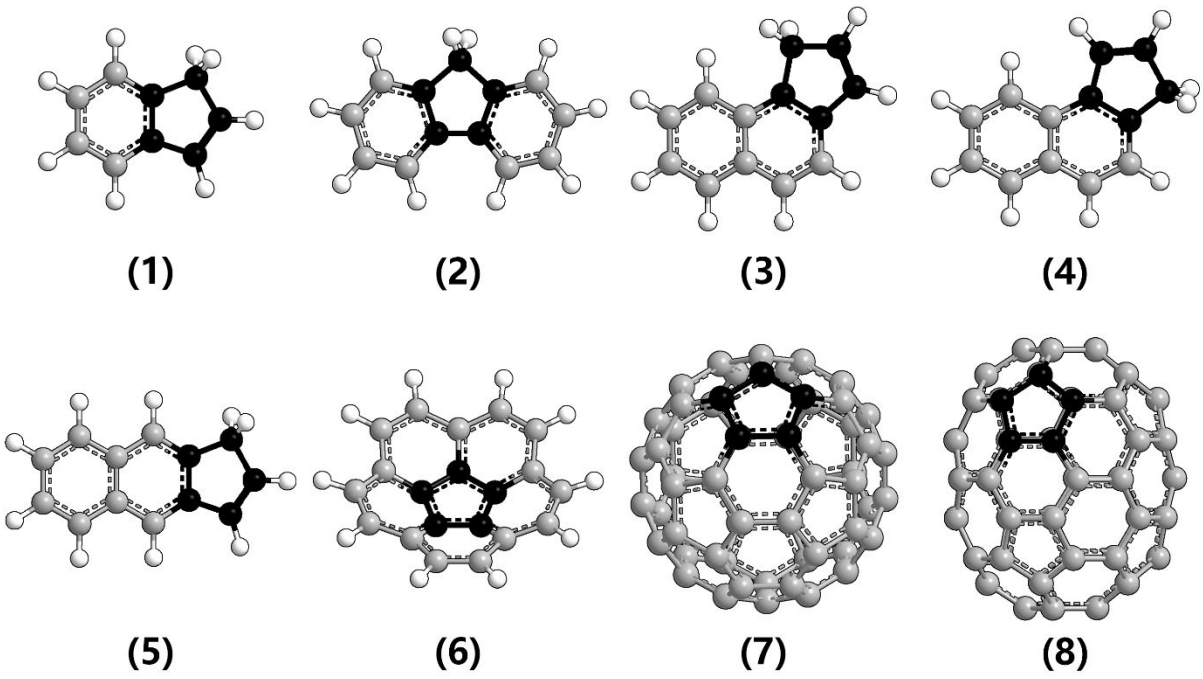

Scheme 1. Molecular building blocks of the 5-member-ring carbon skeleton (black) in indene **(1)**, fluorene **(2)**, 1*H*-cyclopenta[*a*]naphthalene **(3)**, 3*H*-cyclopenta[*a*]naphthalene **(4)**, 1*H*-cyclopenta[*b*]naphthalene **(5)**, corannulene **(6)**, C_{60}-fullerene **(7)** and C_{70}-fullerene **(8)**.

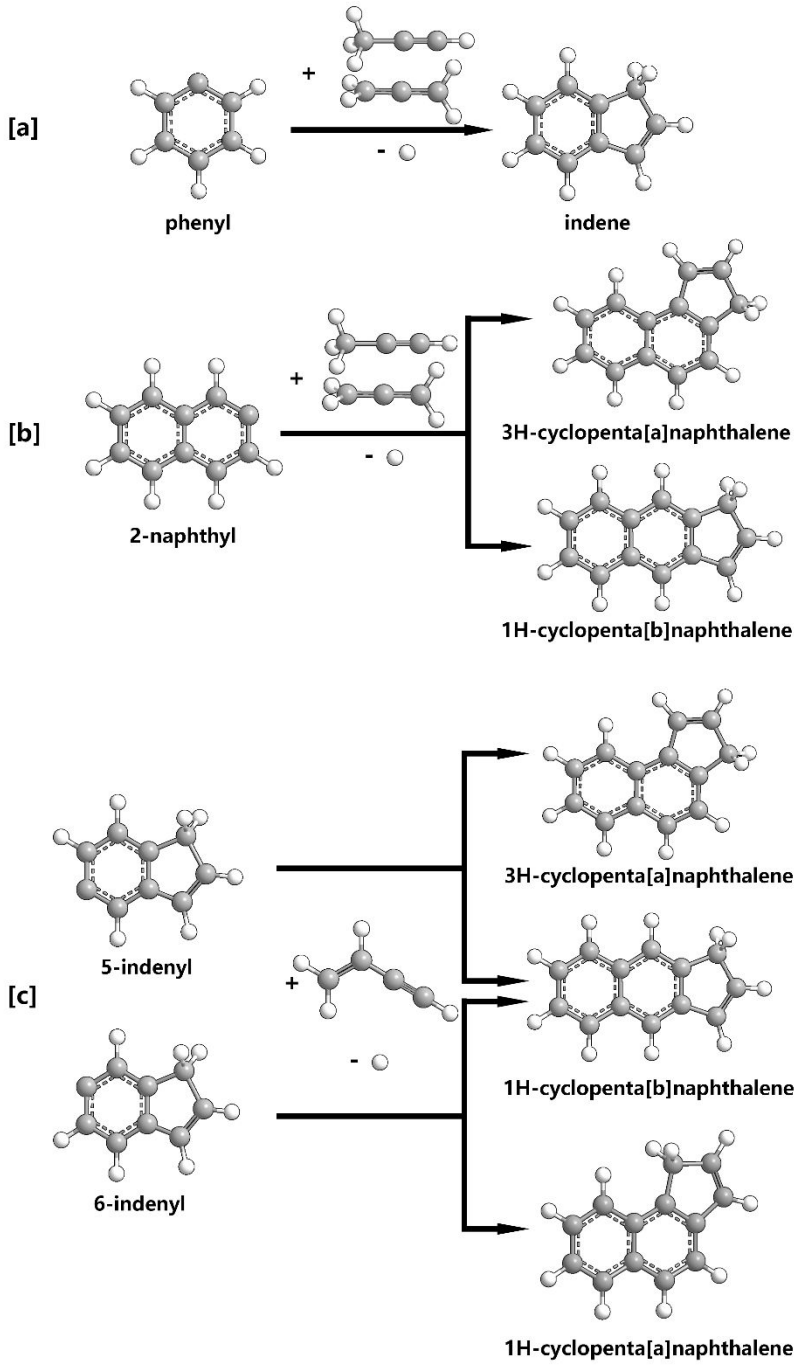

Scheme 2. Reaction schemes: [a] phenyl ($C_6H_5^{\bullet}$) reacts with allene/methylacetylene (C_3H_4) and yields indene;[11] [b] 2-naphthyl ($C_{10}H_7^{\bullet}$) reacts with allene/methylacetylene (C_3H_4) leading to the formation of 3*H*-cyclopenta[*a*]naphthalene/1*H*-cyclopenta[*b*]naphthalene ($C_{13}H_{10}$);[14] [c] 5-/6-indenyl radicals ($C_9H_7^{\bullet}$) is proposed to react with vinylacetylene (C_4H_4) to produce 3*H*-cyclopenta[*a*]naphthalene, 1*H*-cyclopenta[*b*]naphthalene, and 1*H*-cyclopenta[*a*]naphthalene ($C_{13}H_{10}$).

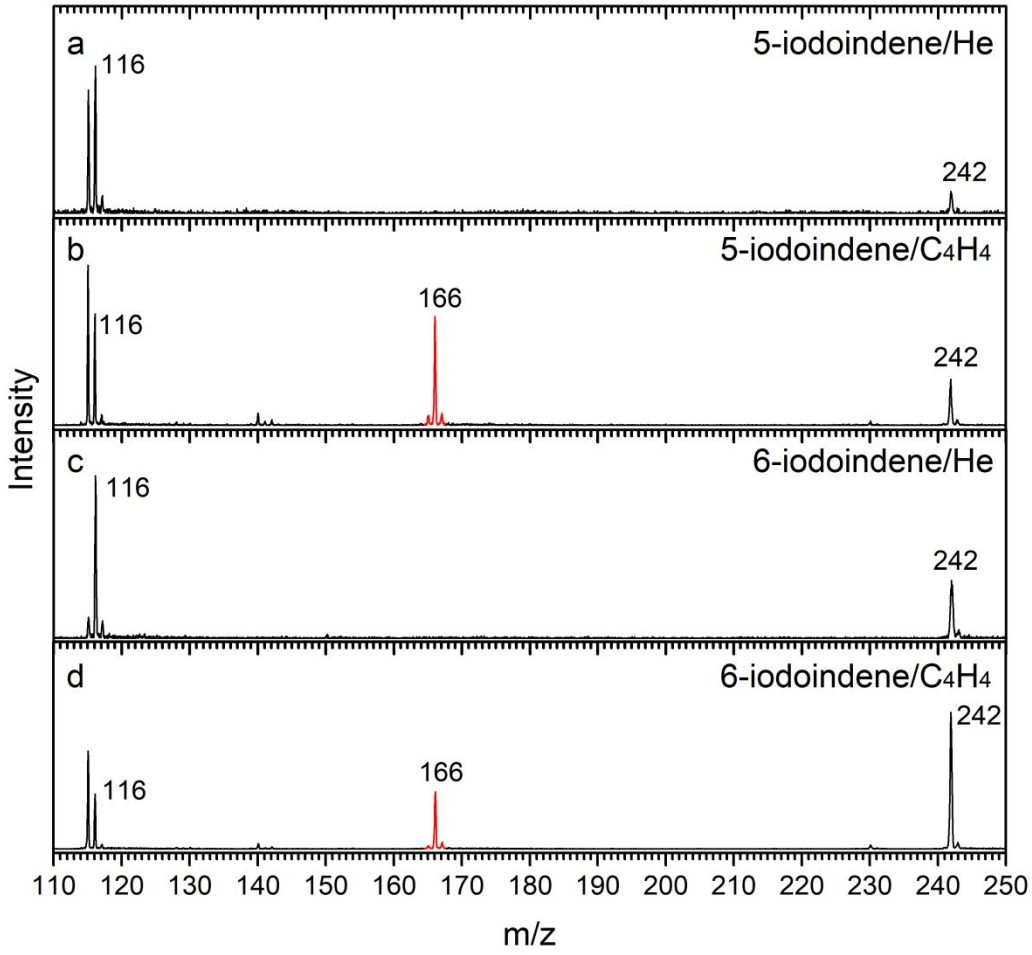

Figure 1. Comparison of photoionization mass spectra recorded at a photon energy of 9.50 eV with the reaction temperature at 1300 ± 10 K. (a) 5-iodoindene (C_9H_7I) – helium (He) system; (b) 5-iodoindene (C_9H_7I) – vinylacetylene (C_4H_4) system; (c) 6-iodoindene (C_9H_7I) – helium (He) system; and (d) 6-iodoindene (C_9H_7I) – vinylacetylene (C_4H_4) system. The mass peaks of the newly formed species along with the ^{13}C-counterparts are highlighted in red.

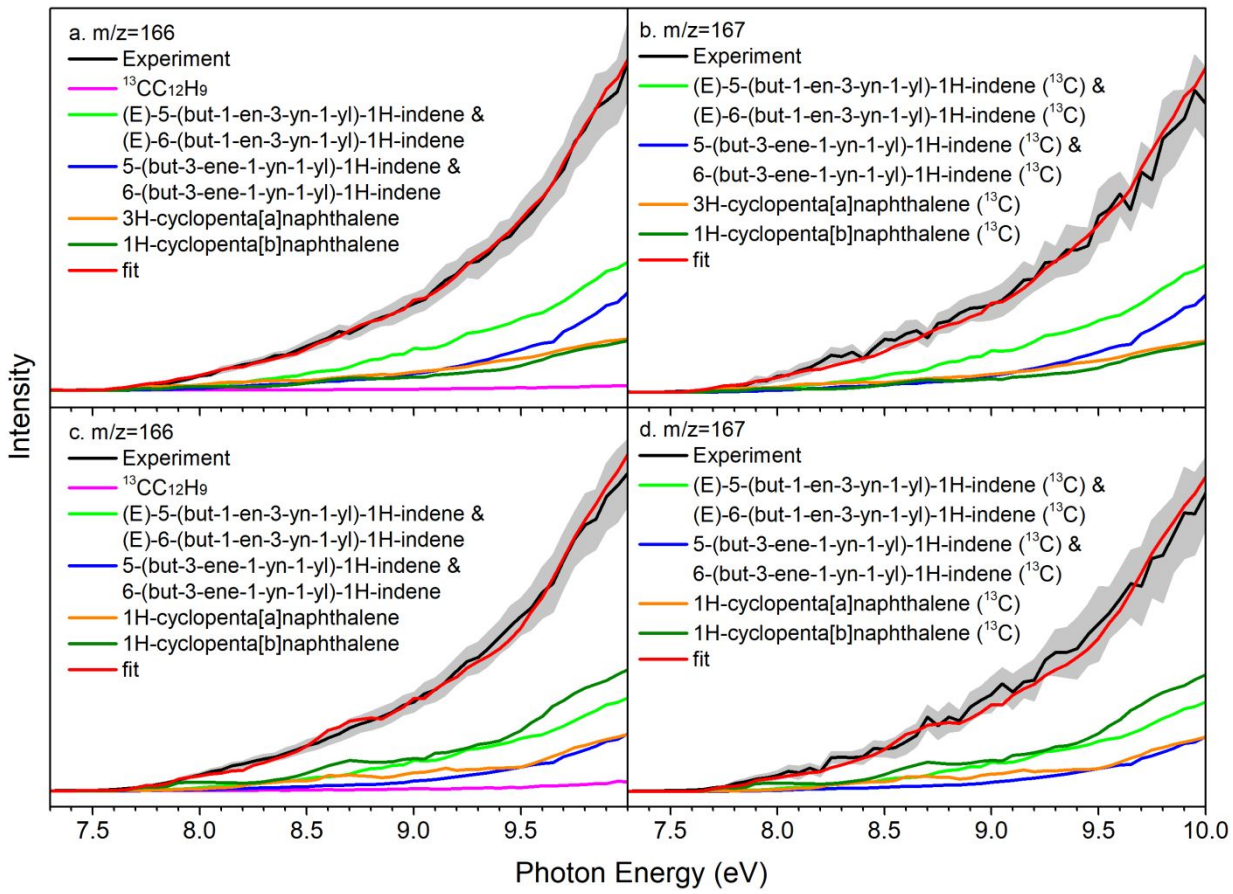

Figure 2. Photoionization efficiency (PIE) curves for signal at *m/z* = 166 and 167 in the reactions of indenyl radicals with vinylacetylene. Upper panels (a and b): 5-indenyl ($C_9H_7^{\bullet}$) + vinylacetylene (C_4H_4); Lower panels (c and d): 6-indenyl ($C_9H_7^{\bullet}$) + vinylacetylene (C_4H_4). Black lines present experimentally derived PIE curves along with the error bars indicated in gray; colored lines (green, blue, olive and orange) present the reference PIE curves; and red lines are the overall fit. The overall error bars consist of two parts: ±10% based on the accuracy of the photodiode and a 1 σ error of the PIE curve averaged over the individual scans.

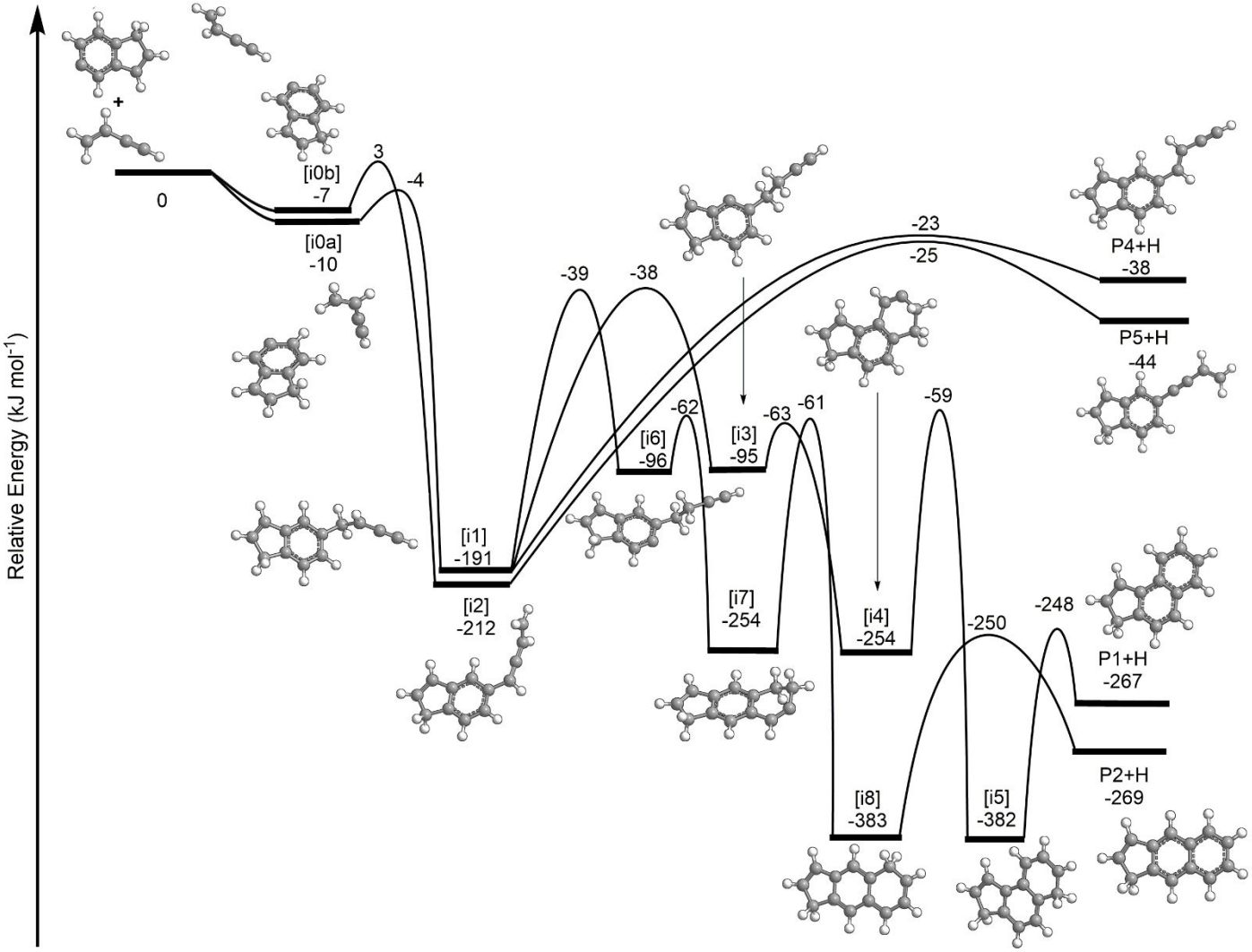

Figure 3. Potential energy surface (PES) for the 5-indenyl ($C_9H_7^{\bullet}$) reaction with vinylacetylene (C_4H_4) leading to the formation of 3*H*-cyclopenta[*a*]naphthalene (**P1**), 1*H*-cyclopenta[*b*]naphthalene (**P2**), (*E*)-5-(but-1-en-3-yn-1-yl)-1*H*-indene (**P4**), and 5-(but-3-ene-1-yn-1-yl)-1*H*-indene (**P5**). The relative energies are given in kJ mol^{-1}.

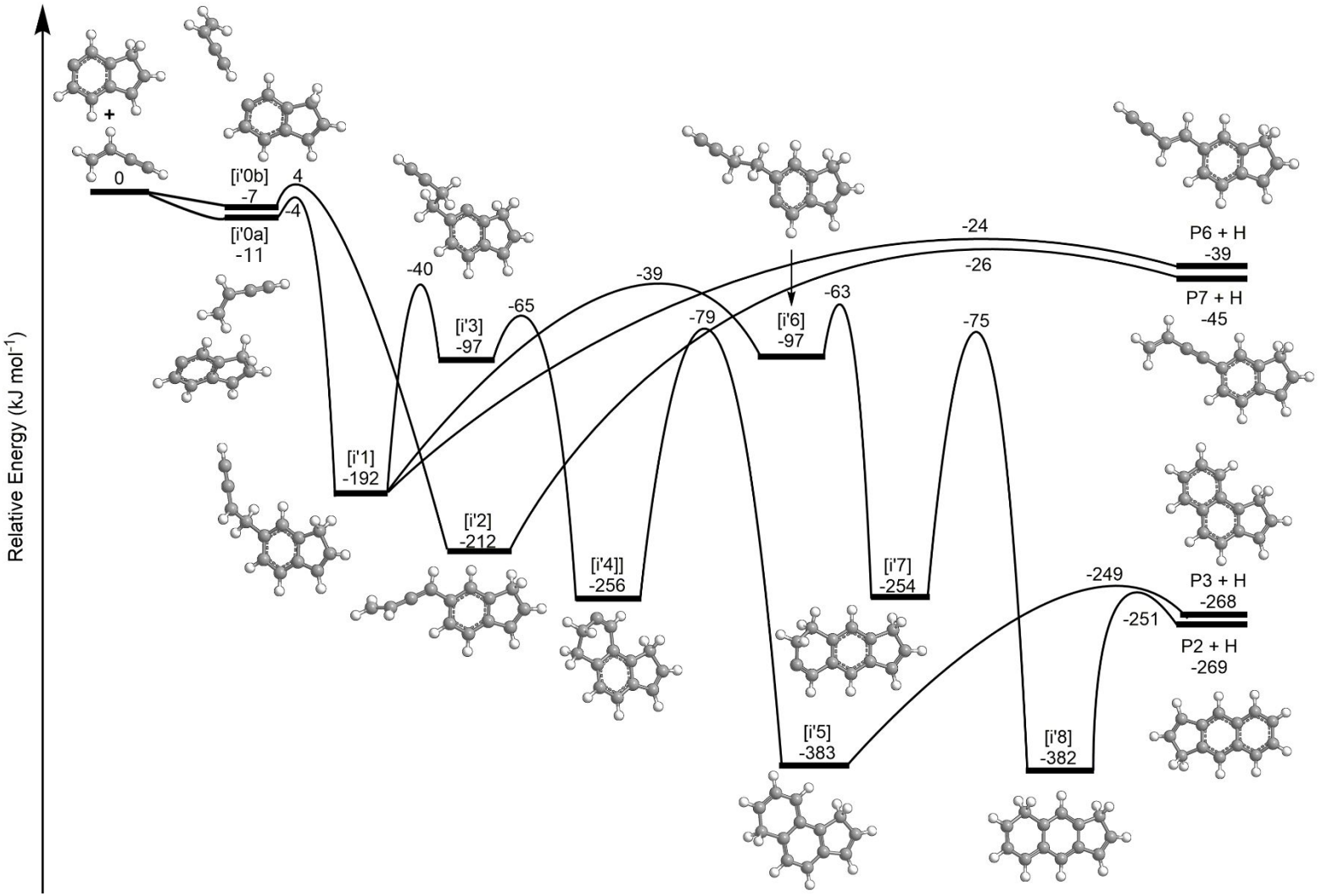

Figure 4. Potential energy surface (PES) for the 6-indenyl ($C_9H_7^{\bullet}$) reaction with vinylacetylene (C_4H_4) leading to the formation of 1*H*-cyclopenta[*b*]naphthalene (**P2**), 1*H*-cyclopenta[*a*]naphthalene (**P3**), (*E*)-6-(but-1-en-3-yn-1-yl)-1*H*-indene (**P6**), and 6-(but-3-ene-1-yn-1-yl)-1*H*-indene (**P7**). The relative energies are given in kJ mol^{-1}.

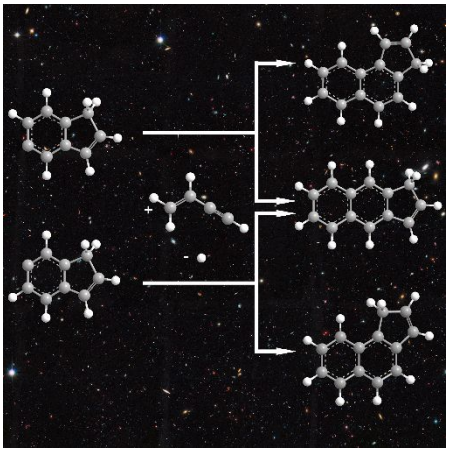

The reaction of indenyl radicals with vinylacetylene leads to cyclopentanaphthalene at low temperature.